Lawrence Livermore National Laboratory

LLNL-TR-670539

Time-Correlated Particles Produced by Cosmic Rays

George Chapline, Andrew Glenn, Les Nakae, Iwona Pawelczak, Neal Snyderman, Steven Sheets, and Ron Wurtz

Lawrence Livermore National Laboratory,
P.O. Box 808, Livermore, CA 94551-0808

6 May 2015

Disclaimer

Lawrence Livermore National Laboratory is operated by Lawrence Livermore National Security, LLC, for the U.S. Department of Energy, National Nuclear Security Administration under Contract DE-AC52-07NA27344.

Time-Correlated Particles Produced by Cosmic Rays

George Chapline, Andrew Glenn, Les Nakae, Iwona Pawelczak,

Neal Snyderman, Steven Sheets, and Ron Wurtz,

Lawrence Livermore National Laboratory

4 June 2015

Abstract

This report describes the NA-22 supported cosmic ray experimental and analysis activities carried out at LLNL since the last report, dated October 1, 2013. In particular we report on an analysis of the origin of the plastic scintillator signals resembling the signals produced by minimum ionizing particles (MIPs). Our most notable result is that when measured in coincidence with a liquid scintillator neutron signal the MIP-like signals in the plastic scintillators are mainly due to high energy tertiary neutrons.

Introduction

The cosmic ray observations carried out at LLNL during the period 2012-2014 were carried out using arrays of 4" x 3" liquid scintillator (LS) cells and 0.4m^2 area x 5.7cm thick plastic scintillator panels. These experiments were initially carried out outdoors in order to eliminate the effects of cosmic rays interacting with the ceiling and walls of a building. At the end of 2013 this array was moved indoors, with the exception that for 2 weeks during the summer of 2014 the liquid scintillator cells and some of the plastic scintillator panels were moved to the White Mountain research station near Bishop, California. Our main interest in carrying out these experiments was to investigate the frequency and nature of time coincident signals in the liquid and plastic scintillators. As discussed in our October 2013 report MIP-like signals in the plastic scintillators were frequently recorded in coincidence with fast neutron signals in the liquid scintillator cells. Furthermore the dependence of the time coincident signals in the liquid and plastic scintillators on the location of the plastic scintillators clearly showed that the particles producing the MIP-like signals were coming from the

Pb pile. One of our main focuses in FY14 was to try to identify the types of tertiary particles responsible for these coincident MIP-like signals. At the time of our previous report, we were not able to report the relative contribution of the various types of tertiary particles that may have been responsible for the coincident MIPs-like signals in the plastic scintillators. We did report the results of Monte Carlo simulations of the numbers of tertiary muons, pion, and protons hitting the plastic scintillators, but we omitted predictions for the numbers of tertiary neutrons hilling the plastic scintillators, partly because we didn't have a model for how a fast neutron would interact with the plastic scintillators. In addition we were unable to devise a simple experimental technique for distinguishing the different types of particles hitting these detectors.

In 2014 we carried out extensive Monte Carlo simulations of the atmospheric showers produced by primary cosmic rays, and the subsequent interaction of the secondary particles in these cosmic ray showers with materials at sea level. In general these simulations have provided a good understanding of the observations of the tertiary particles resulting from secondary cosmic ray interactions with piles of Pb bricks. Our Monte Carlo simulations of the interactions of tertiary protons, neutrons, and pions with our plastic scintillator panels are now in reasonable agreement with the rates of coincident signals observed in our liquid and plastic scintillator detectors.

Unfortunately we were not able to experimentally check the Monte Carlo predictions for the relative contributions of various types of tertiary particles to the coincident plastic scintillator signals. However, our Monte Carlo simulations of interaction of secondary cosmic ray particles with Pb piles have provide valuable insights into a number of the puzzles dating back to our 2006 experiments. In particular, it is now clear that cosmic ray induced bursts in Pb piles can indeed contain very large numbers of neutrons and occur unexpectedly often. In addition it now appears that a significant fraction of the multiple neutron busts produced in high Z materials by cosmic rays are due to primary cosmic ray protons which penetrate to an altitude of few kilometers above sea level before undergoing significant interactions with the atmosphere. Another surprising observation dating back to 2006 was the observation of muon-like signals in plastic muon detectors occurring in coincidence with the cosmic ray induced bursts of neutrons. As

discussed in more detail in the section on Monte Carlo simulations, our Monte Carlo calculations of the rates with which various types of tertiary particles hit the plastic scintillator array does explain the multiple MIP-like signals seen in coincidence with LS signals. In particular, the Monte Carlo simulations imply that the coincident MIP-like signals in the plastic scintillator detectors are mainly due to tertiary neutrons with energies exceeding 20 MeV.

An expected strong increase in the production of large neutron bursts in high Z materials at altitudes of a few kilometers was our main motivation for moving our liquid and plastic scintillators to the White Mountain Research Station at an altitude of 4 km. During a 2 week observing period in August, 2014 we obtained data on both the cosmic ray neutron background at this altitude as well as the neutron bursts produced by relatively small amounts of lead. We have not yet carried out Monte Carlo simulations of the White Mountain experiments, but will include an analysis of this data in our next report.

LLNL experiments

The experiments that we carried out in 2013-14 initially used an array of 74 4" diameter x 3" long liquid scintillator (LS) cells and 18 1m x 0.4m x 5.7cm plastic scintillator "muon panels" (see picture below). The liquid scintillators were intended to record fast neutrons, while the plastic scintillators were intended to record signals from minimum ionizing particles such as cosmic ray muons. In our experiments these detectors were almost always placed close together, while leaving a space in the middle where a 50cm x 50 cm x 50 cm Pb pile could be placed. The signals from both the liquid and plastic scintillators were simultaneously recorded in a multi-channel pulse digitizer with a time stamp on each pulse that was accurate to a few nanoseconds. The plastic scintillator panels were laid out on the ground with the packs of liquid scintillator cells placed on top of the plastic scintillators as shown in Figures 1 and 2. Figure 2 shows the arrangement of detectors used outdoors in 2013 to study the dependence of the coincident MIP-like signal rate on distance from the Pb pile.

Figure 1: Detector system deployed outdoors at LLNL during 2012-2013. Initial layout consisted of 18 muon panels laid flat on the ground and covering approximately 6 square meters, together with 76 liquid scintillators placed on top. The detectors were connected by cables with a high voltage supply for the liquid scintillators and digital data acquisition and storage system as shown.

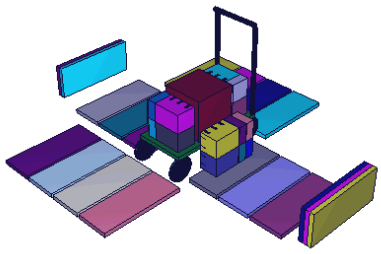

Figure 2: Geometric model used for simulating the production of the tertiary cosmic ray particles from a 1 ton Pb pile. The Pb pile was placed on top of a 24”x24” cart.

In both our outdoor and indoor experimental set-ups a space was left in the center of the array of plastic and liquid scintillators to accommodate a 24”x24” cart, which was able to hold about 1 ton of Pb bricks as shown in Fig. 2. The measurements of the cosmic ray signals in the liquid and plastic scintillators carried out outdoors in 2013 and indoors in 2014 were carried out both with and without the presence of the pile of Pb bricks on the cart.

These measurements confirmed our earlier observations with ^{3}He detectors that a Pb pile produces correlated bursts of neutrons on the order of once a minute. Fig. 3 is a “waterfall plot” showing the time interval between successive neutrons, gammas, and muons measured with the liquid scintillator array and plastic panels shown in Fig. 1 as a function of time for 5 days of data. The occurrence of very large neutron bursts is less evident in this data than in the 2007 data obtained with He3 counters because of the lower efficiency of our liquid scintillator array. Fig. 4 is a “Ron” plot obtained by projecting only the neutrons in the waterfall plot onto the y-axis, which shows the statistical distribution of time intervals between successive LS neutron counts. It can be seen that in addition to the band of time intervals longer than a microsecond, which largely represent an uncorrelated background, there is a strong band of time intervals on the order of several nanoseconds which represent bursts of time correlated fast neutrons. Fig. 5 shows the multiplicity distribution for bursts of LS neutrons. These neutrons have energies in the range ~ 1 to 10 MeV.

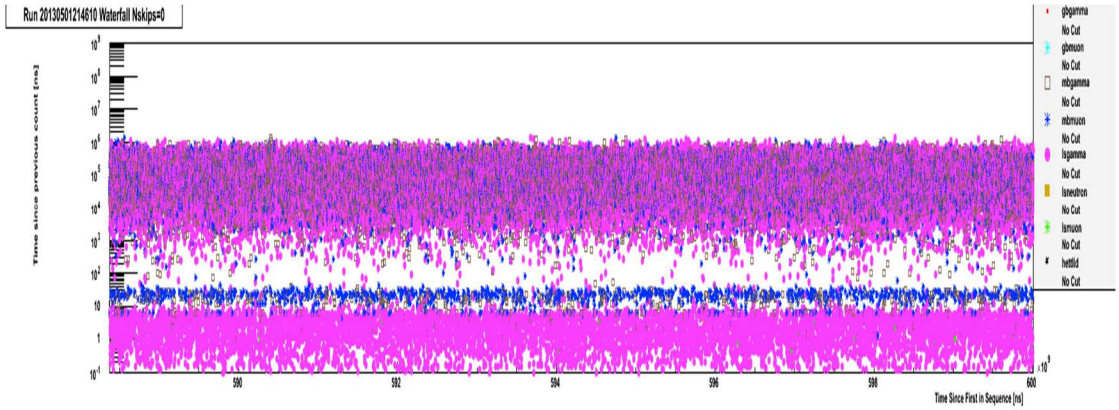

Figure 3: Time intervals between fast neutrons (gold), gammas (pink), and muons (blue) observed during a 4.5 day period.

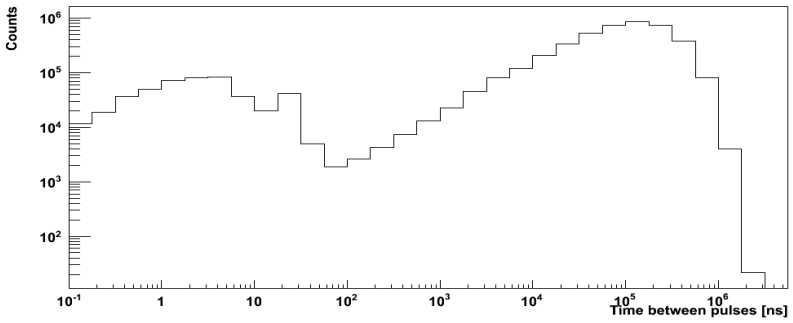

Figure 4: Distribution of time intervals between LS neutrons observed during a 4.5 day period.

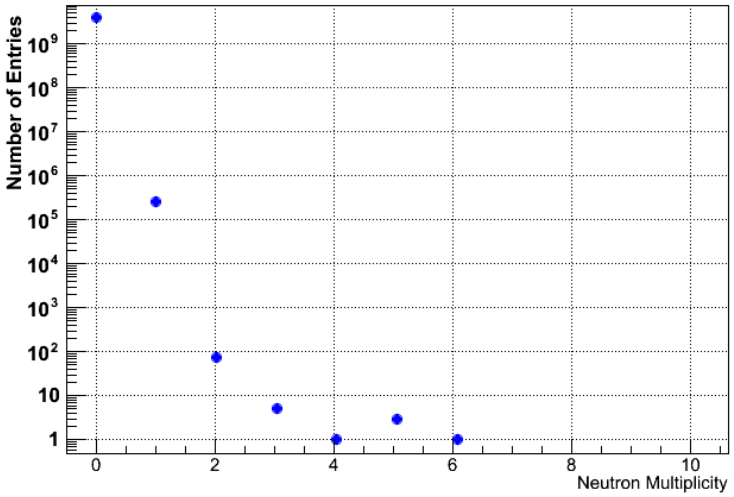

Figure 5: Multiplicity distribution for LS neutrons observed during an 8 hour period.

In Figs. 6-7 we show the observed rates for cosmic ray bursts containing multiple liquid scintillator neutron and plastic scintillator MIP-like signals, with and without the presence of a Pb pile.

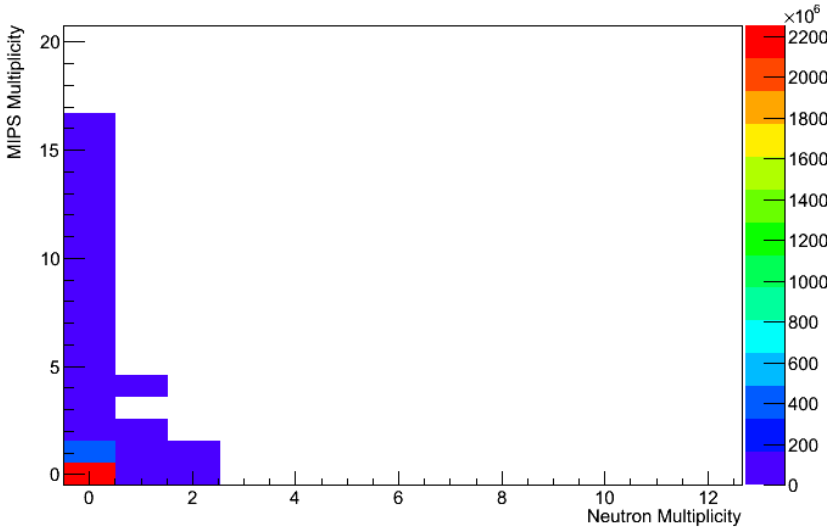

Fig. 6. Observed outdoor rates for LS neutron and/or plastic scintillator MIP-like bursts in the absence of a Pb brick pile for 5.33 days of data.

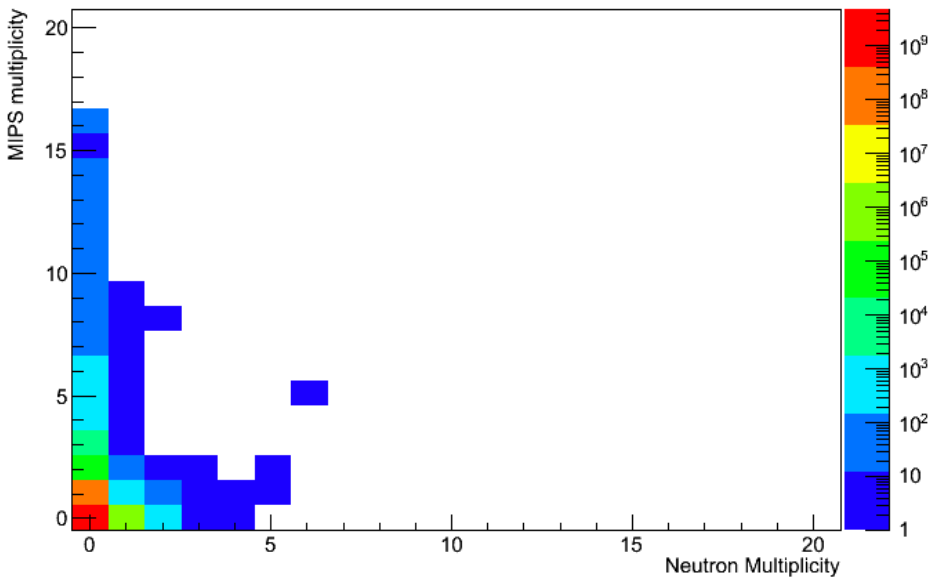

Fig. 7. Observed outdoor rates for bursts containing LS neutron and/or plastic scintillator MIP-like signals in the presence of our 50cmx50cmx50cm Pb brick pile for 5.33 days of data.

The array shown in Fig 1 was moved indoors in the fall of 2013, and we obtained data there on the neutron bursts produced in both liquid scintillators and ^{3}He counters by Pb bricks surrounded by an array of liquid scintillator cells and ^{3}He counters. placed on the 24" x 24" cart shown in Fig 2. The liquid scintillator array consisted of 38 cells placed on opposite sides of the cart in much the same manner as shown in Fig. 2, while the ^{3}He counters were placed along the other two sides. Figs 8-9 show the multiplicity distributions for cosmic ray induced bursts in the Pb bricks as measured in the liquid scintillator and ^{3}He counter arrays. As is evident from the figures, while the presence of a 1 ton Pb makes a noticeable difference in the rate of production of large bursts, it is difficult to distinguish the presence of only a few Pb bricks against background. In Figs 10-11 we show the overall neutron rate depends on the amount of Pb.

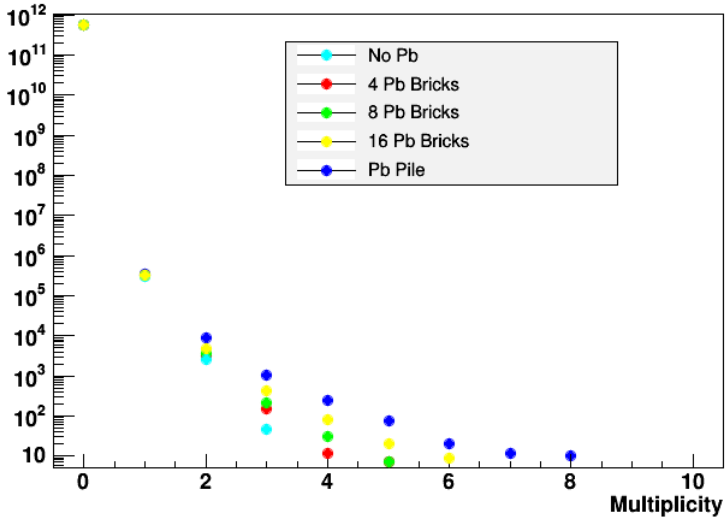

Fig. 8. Observed multiplicity distributions for liquid scintillator neutron bursts in the presence of 4, 8, and 16 bricks as well as our 1 ton Pb pile for 20 hrs of data.

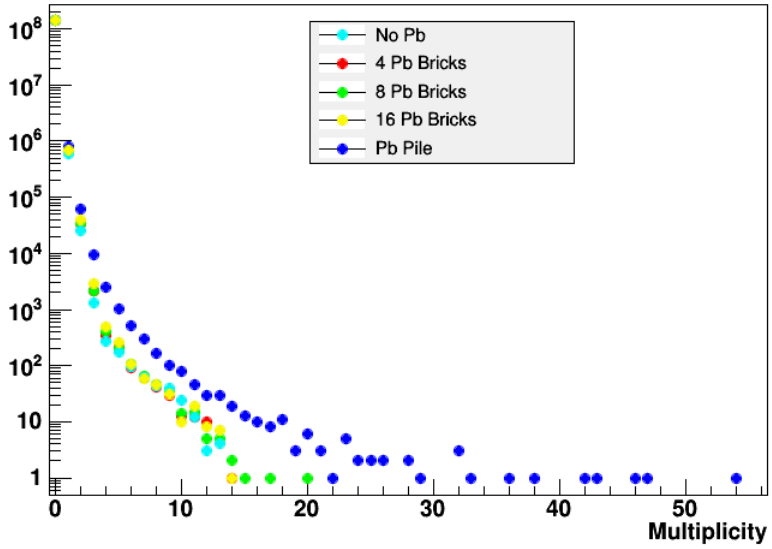

Fig. 9. Observed multiplicity distribution for He3 counter neutron bursts in the presence of 4, 8, and 16 bricks as well as our 1 ton Pb pile for 20 hours of data.

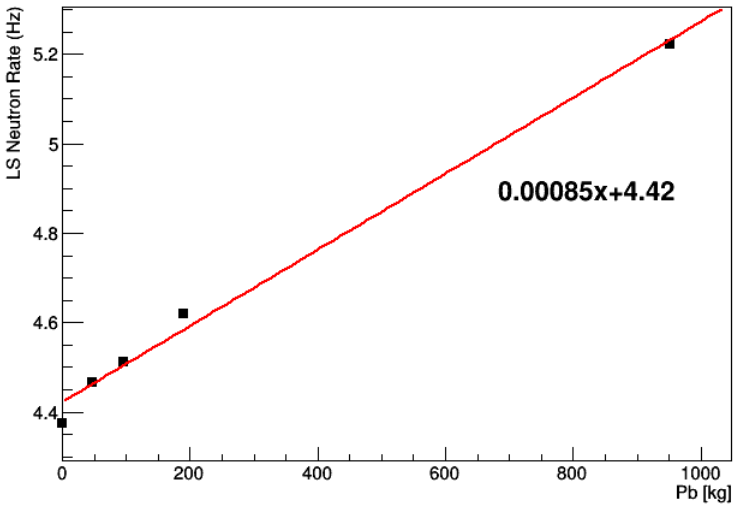

Fig. 10. Interpolated rate liquid scintillator neutron signals as a function of the amount of Pb for 20 hours of data.

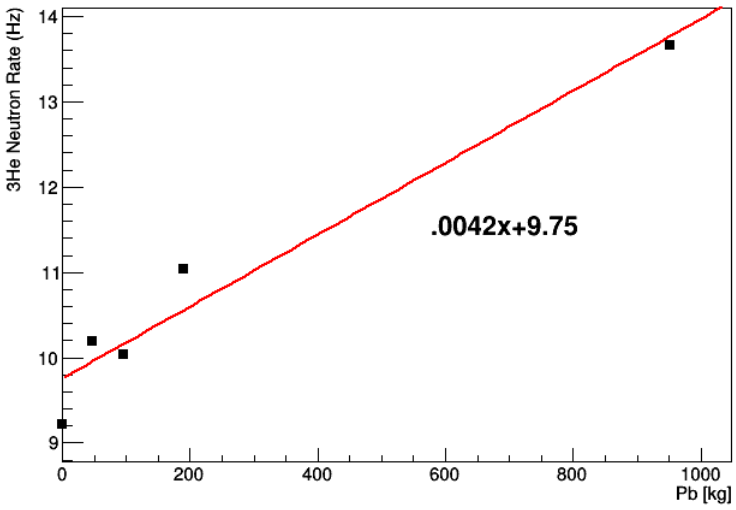

Fig. 11. Interpolated rate for ^{3}He counter neutron signals as a function of the amount of Pb for 20 hours of data.

The indoor rates for coincident bursts of LS neutrons and plastic scintillator MIP-like signals are shown in Figs. 12-13. As is evident from comparing these figures with Figs. 6-7 the outdoors and indoors MIP multiplicities are not too different, while the LS neutron multiplicities appear to be higher indoors.

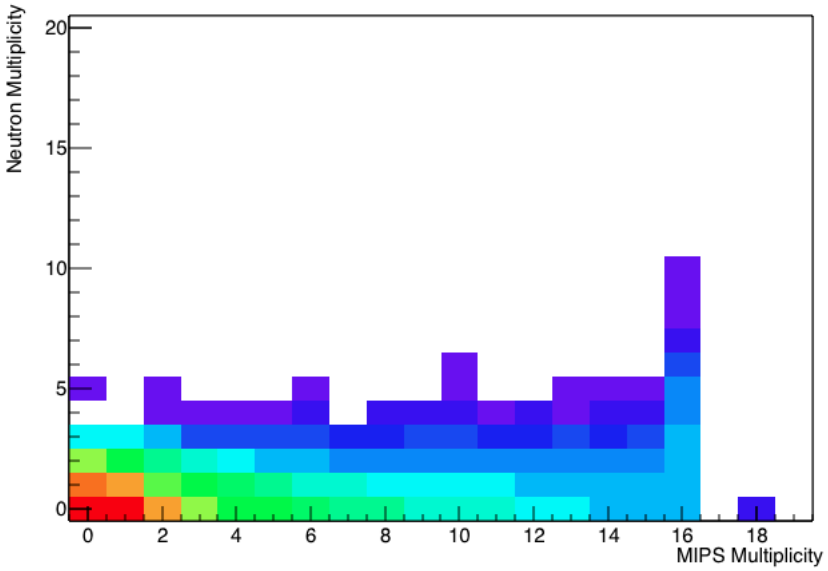

Fig. 12. Observed indoor rates for correlated LS neutron and plastic scintillator MIP-like bursts in the absence of a Pb brick pile for a 20 hour run..

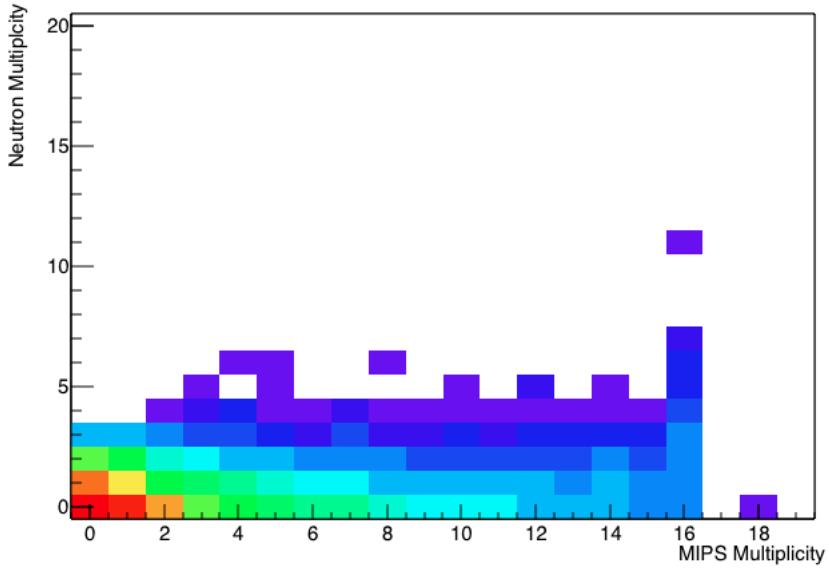

Fig. 13. Observed indoor rates for LS neutron and plastic scintillator MIP-like bursts in the presence of a Pb brick pile for a 20 hour run.

Analysis of experiments carried out at LLNL

Figure 14 shows the predicted multiplicity distribution for tertiary neutrons produced by the sea level cosmic ray particles hitting the Pb pile. This prediction was obtained using the GEANT4 Monte Carlo particle propagation code and the CRY online cosmic ray model for the sea level fluxes of secondary cosmic ray particles. The CRY model predicts that cosmic ray bursts containing hundreds of neutrons will occur several times a day.

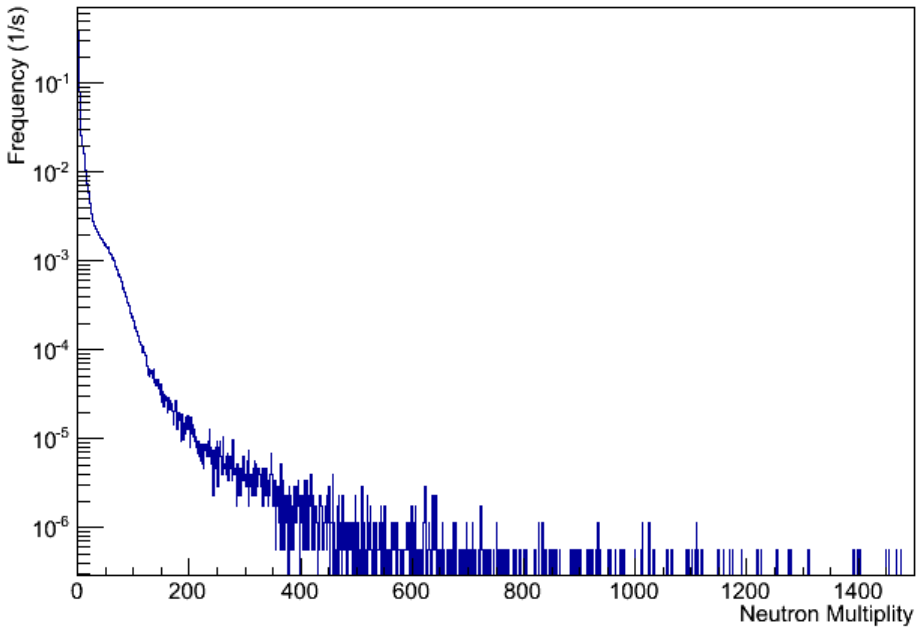

Fig. 14 Monte Carlo prediction for the multiplicity distribution of tertiary cosmic ray neutrons resulting from secondary cosmic rays hitting a 1 ton Pb pile.

The observed distribution does not exhibit the predicted long tail of very large bursts due to the limited efficiency of the liquid scintillator array. In Figure 15 we show the predicted tertiary neutron multiplicity distribution convoluted with a detector efficiency of either 10% or 1%. It can be seen that the observed distribution more closely resembles what would be expected if the effective detector efficiency was about 1%. We believe that the actual efficiency of our liquid scintillator array for detecting for MeV neutrons from the Pb pile is a few percent. The fact that the effective efficiency appears to be close to 1% is apparently due to the fact that many of the tertiary neutrons have energies above 10 MeV, where the intrinsic efficiency of the liquid scintillators is significantly reduced due to the decrease in the neutron-proton scattering cross-section for neutron energies above 10 MeV [Lock and Measday, *Intermediate Nuclear Physics* (Methuen 1970)]. However, as we shall presently see, the decreased efficiency in liquid scintillators for detecting neutrons with energies > 10 MeV is to some extent compensated in our detection system by an increase in the efficiency for detecting neutrons with energies > 10 MeV in our plastic scintillators.

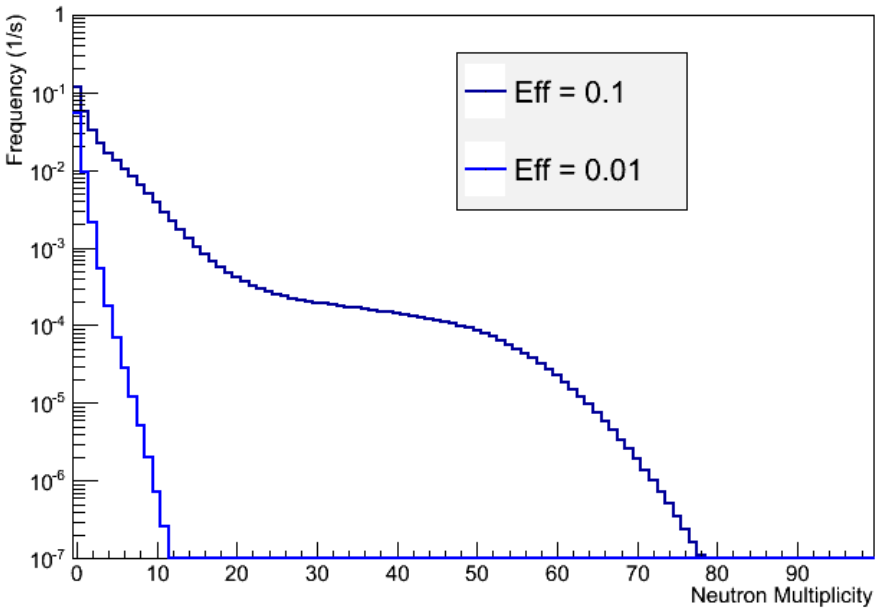

Fig. 15. Predicted neutron multiplicity distribution for tertiary cosmic ray neutrons convoluted with a detector efficiency of either 10% or 1%.

In Figs. 16-17 we show the energy spectra of tertiary particles produced in a 1 ton Pb pile by typical cosmic ray particles (Fig. 16) and by the secondary cosmic particles produced by primary cosmic ray protons with energies greater than 1 TeV (Fig. 17). As expected the spectra for tertiary particles produced by very high energy primary cosmic ray particles is noticeably harder than the spectra of tertiary particles produced by typical cosmic ray secondaries. This is noteworthy because, as mentioned in our previous report, very high energy primaries play a significant role in the generation of neutron bursts with large numbers (viz. hundreds) of neutrons.

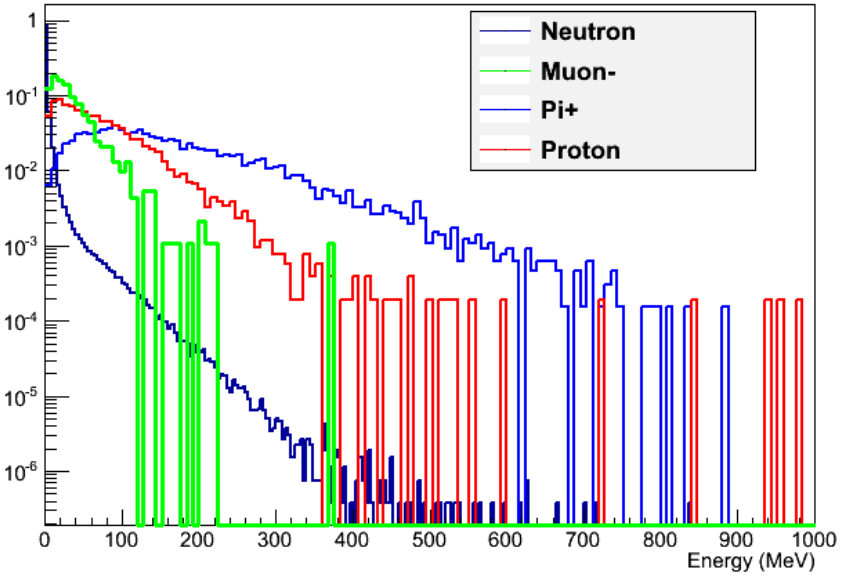

Fig. 16. Monte Carlo prediction for the energy spectra for tertiary neutrons, protons, pions and muons produced in a 1 ton Pb pile. The yields of particles per proton produced are muons: 0.17, pions: 1.26, and neutrons 463.

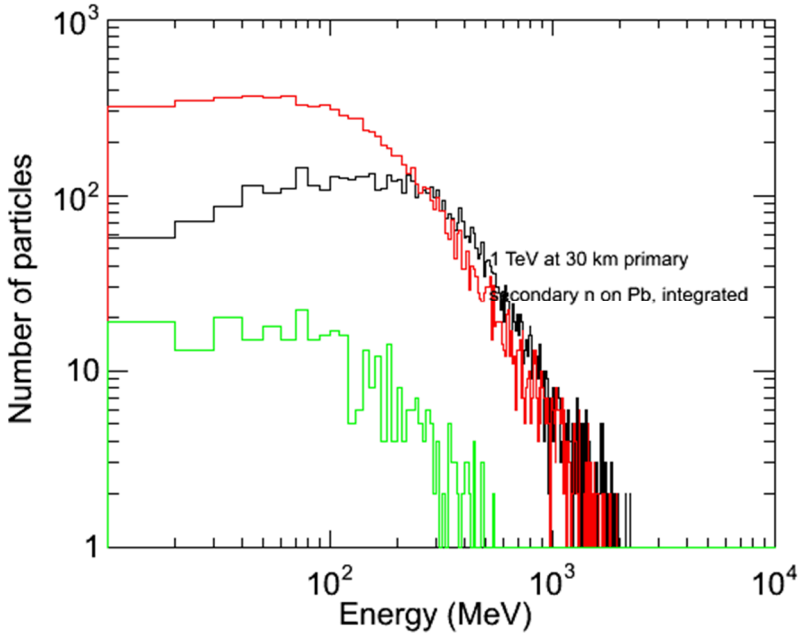

Fig. 17. Monte Carlo prediction for the energy spectra of tertiary neutrons, protons, pions and muons produced by secondary cosmic ray neutrons resulting from primary cosmic rays hitting the top of the atmosphere with energies above 1 TeV. Red = ? black = ? green = ?.

Config	Gamma	Neutron	Proton	Mu-	Mu+	Pi-	Pi+	e-
With Pb	12.3	24.3	8.07	211.6	4.6	.1	.07	1.4
No Pb	1.9	21.5	8.2	208.6	.56	.09	.06	.2
No Pb or ground	1.9	21.4	8.2	208.7	.6	.08	.07	.2

Table 1. Predicted rates for cosmic ray particles hitting the plastic scintillator panels in the detector array shown in Fig 2.

Predictions for rates with which various the various types of cosmic ray particles hit our array of plastic scintillators are shown Table 1. It can be seen that the presence of the ground makes little difference. However, the rates are modestly higher in the presence of the 1 ton Pb pile due to the tertiary particles produced in the Pb pile. These rates were calculated using the GEANT4 Monte Carlo particle propagation code and the CRY library model for the cosmic ray flux at sea level. The most common events represent solitary secondary cosmic ray muons produced by primary high energy protons hitting the top of the atmosphere. Only a fraction of these particles are detected because the plastic scintillator events are recorded only if the light output corresponds to a minimum energy particle depositing 10 MeV or more. In the case of cosmic ray muons this fraction is close to 100% because their energies are typically on the order of a GeV. However, in the case of neutrons hitting the plastic scintillators only neutrons with energies greater than about 20 MeV would be recorded, because only for these energetic neutrons would the recoil proton in the plastic have sufficient energy to deposit the threshold energy of 10 MeV. In Fig. 18 we show the rate with which neutrons with a kinetic energy energy greater than 20 MeV hit our detector array together with the incidence rates for other types of cosmic ray particles.

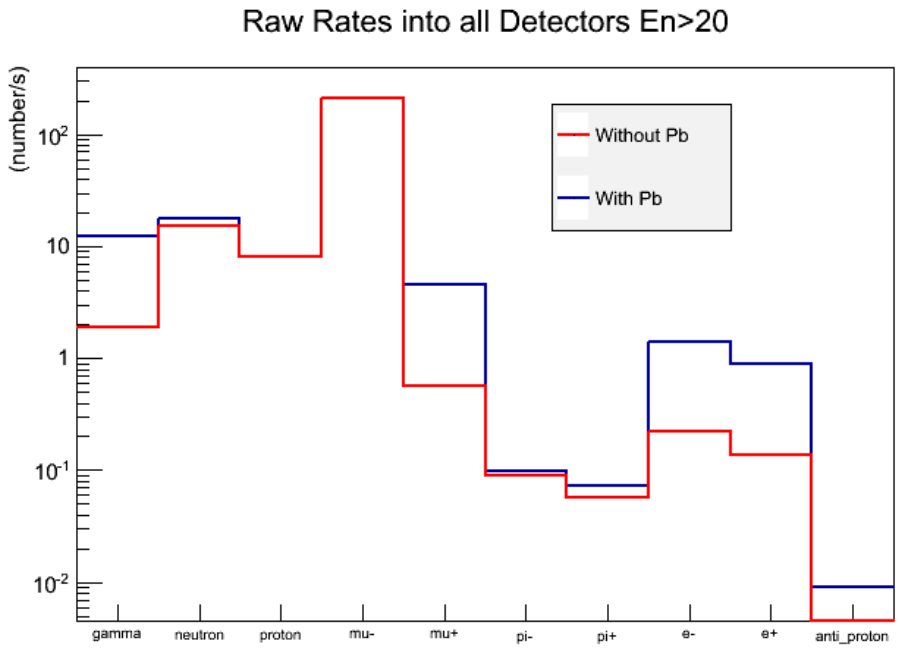

Fig. 18. Predicted rate for cosmic ray neutrons with kinetic energies > 20 MeV particles hitting our detector array compared with the incidence rate for other types of cosmic ray particles.

As is evident from Fig. 18 neutrons with a kinetic energy greater than 20 MeV constitute a significant fraction of all the neutrons hitting our detector array. This fraction becomes even more significant when coincidences between liquid scintillator neutron signals and MIP-like signals in the plastic scintillator are considered.

Config	Gamma	Neutron	Proton	Mu-	Mu+	Pi-	Pi+	e-
With Pb	0	1.05	.009	0.02	0	0	.003	0
No Pb	0	0.28	.003	0.015	0	0	0	0
No Pb or ground	0	0.30	.001	0.012	0.06	0	0	0

Table 2. Monte Carlo predictions for the rates at which cosmic ray particles hit our detector array within 100 ns of a liquid scintillator neutron signal.

In Table 2 we show the incidence rates for cosmic ray particles which are closely time correlated with a LS neutron signal. Obviously these rates are significantly lower than the rates shown in Table 1. What is

particularly striking though is that the correlated incidence rates are dominated by neutrons rather than muons. In Fig. 19 we show how the coincident incidence rates compare when the kinetic energy of the neutron is restricted to be greater than 20 MeV.

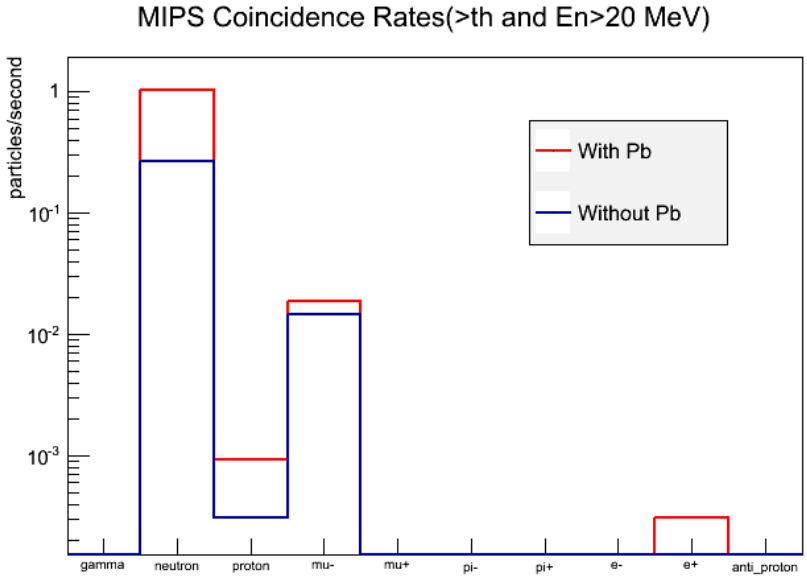

Figure 19. Predicted rates for tertiary cosmic ray particles hitting a plastic scintillator panel in our detector array within 100ns of a LS neutron signal. The kinetic energy of the cosmic ray neutrons was restricted to be > 20 MeV.

It can be seen that, in contrast with the average fluxes of cosmic ray particles shown in Fig. 18, the rate of coincidences between LS neutron signals and MIP-like plastic scintillator signals is predicted to be completely dominated by tertiary neutrons with energies > 20 MeV. Part of the reason for this dominance is that the spectrum of tertiary cosmic ray neutrons hitting the plastic scintillators in the presence of the Pb pile peaks near to ~ 100 MeV. In Fig. 20 we show the spectrum of all neutrons hitting the plastic scintillator within 100ns of an LS neutron detection. As noted above only neutrons with kinetic energies > ~ 20 MeV will produce a MIP-like signal in our plastic scintillator detectors. However, as is evident from Fig 20 most of neutrons that are generated in the Pb pile and hit the plastic scintillator array will have kinetic energies > 20 MeV. This result is consistent the long known fact [Hess et. al. Phys. Rev. 116, 445 (1959)] that the spectrum of neutrons in the atmosphere has a peak near to 100 MeV.

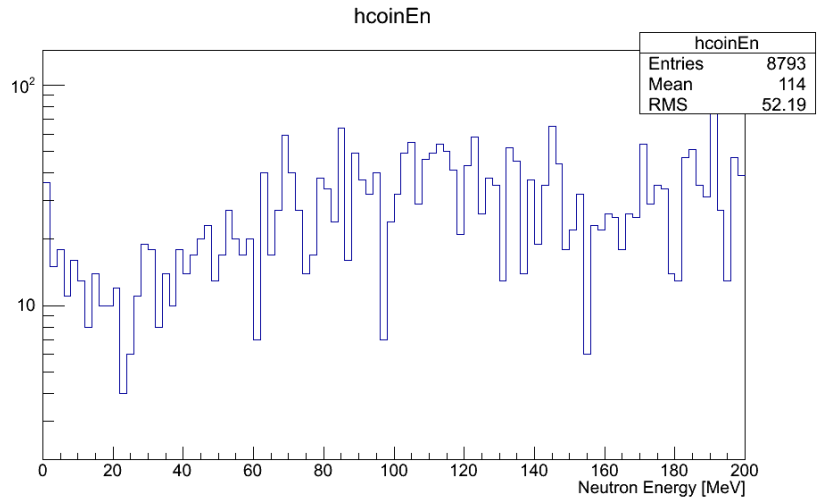

Fig. 20. Monte Carlo prediction for the spectrum of cosmic ray neutrons hitting a plastic scintillator panel in our array within 100ns of a LS neutron detection.

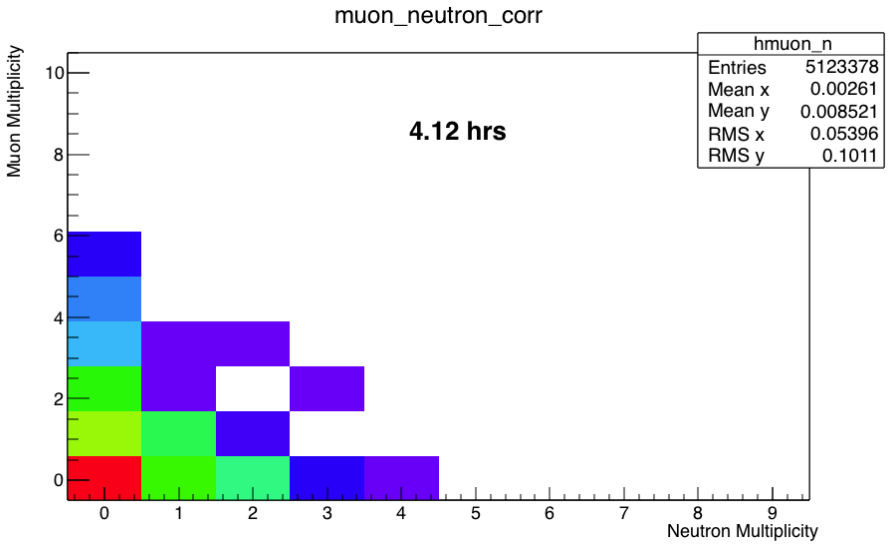

Fig. 21. Multiplicities of secondary neutrons and muons in cosmic ray showers hitting a 1m^2 area of the ground, calculated using the online CRY cosmic ray library.

Fig, 21 shows the frequency with which multiple numbers of secondary neutrons and muons cross a 1 m^2 area of ground calculated using the CRY online cosmic ray library. Although bursts containing many neutrons and muons are expected to be relatively rare, there do appear to be secondary cosmic ray events containing at least 2 neutrons and 2 muons. Whether this is physically correct is unclear because previous

Monte Carlo simulations of single cosmic ray showers that we had carried out (see previous report) had shown that the neutrons and muons in single showers are typically separated by hundreds of meters. In Figure 22 we show our Monte Carlo predictions for the rates for events in our detector array which contain multiple LS neutron and/or plastic scintillator MIP-like signals when no Pb pile is present. These predictions were obtained using a model for the efficiency with which various types of particles hitting our liquid and plastic scintillators are detected. In particular our model only neutrons with kinetic energies in a range between 0.5 MeV and 10 MeV will be readily detected in our LS array, while only neutrons with energies > ~ 20 MeV will be readily detected by the plastic scintillators.

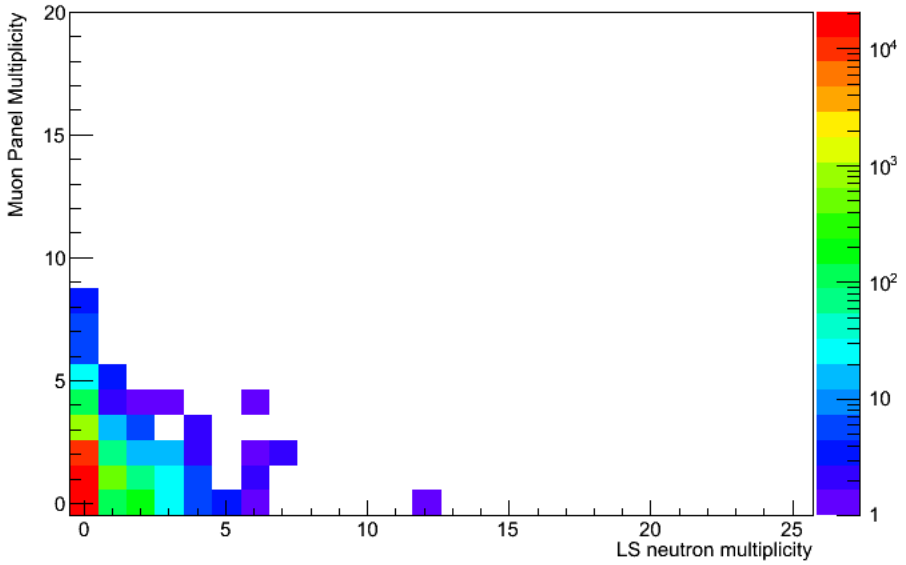

Fig. 22. Predicted Monte Carlo rates for events with multiple LS neutron signals and/or plastic scintillator MIP-like signals in the absence of a Pb pile for 2 hours of real time..

In Fig. 23 we show our predicted rates in the presence of the 1 ton Pb pile. It is evident that the presence of the Pb pile should strongly enhance the number of number of LS neutrons in events with both LS neutron and MIP-like plastic scintillator signals.

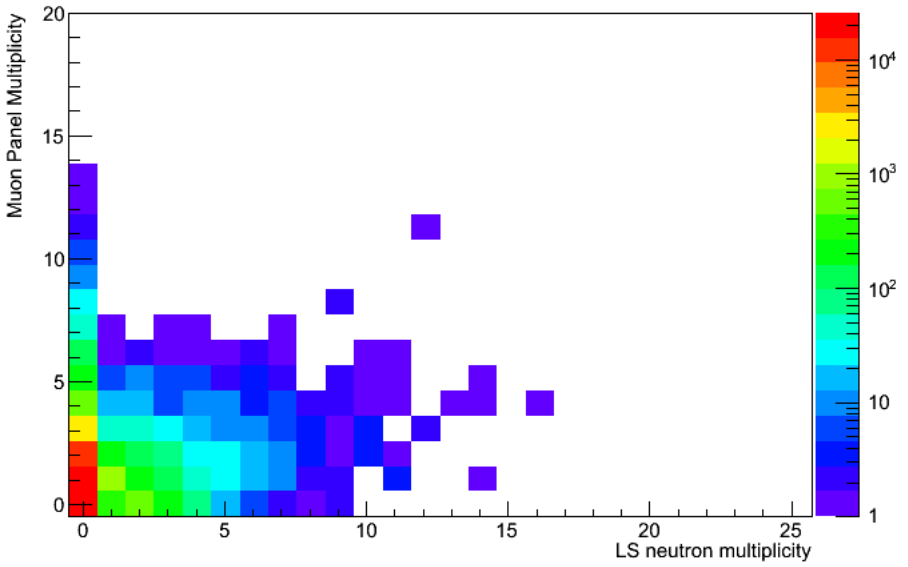

Fig. 23. Monte Carlo rates for events containing multiple LS neutrons and/or plastic scintillator MIP-like signals in the presence of a 1 ton Pb pile for 2 hours of real time.

..

White Mountain Experiments

In July, 2014 we transported 74 of the liquid scintillator cells and 10 of the plastic scintillator panels used in our LLNL experiments to the University of California White Mountain Research Station located at 12,400 feet (3780 meters) in the White Mountains just east of Bishop, California. Over a two week period we carried out a series of observations of the cosmic ray background at this location in the presence of varying amounts of Pb. The liquid and plastic scintillators along with our multi-channel data acquisition system were transported to White Mountain in two Ford pick-up trucks. During the experimental runs the bed of one of these pick-up trucks was used to hold the liquid scintillators and the Pb bricks used in the experiments. The plastic scintillators were placed on the ground beneath the trucks, while the data acquisition system was used placed on the ground next to the truck (see Fig.s 24-29). All the liquid and plastic scintillators survived the trip to the research station even though the last 25 miles of the journey was over a very bad road that often causes flat tires. That all our detector channels were operational after transport over this road is a good omen for the eventual use of liquid scintillator neutron detectors in field operations.

The experiments were carried out over a period of 2 weeks, with approximately 4 days devoted to observations of the cosmic ray background, and the remainder of the time devoted to observations of of the background in the presence of 2 Pb bricks, 4 Pb bricks and a pile of Pb bricks weighing approximately 500lb. Two Pb bricks weigh approximately 23 kg, and so approximate a threat quantity of a fissile material such as Pu239 or U235.

Fig. 24. Experimental set-up at the White Mountain Research station showing the liquid scintillators in the truck bed, the plastic scintillators beneath the truck bed, and the cables connecting the detectors to the DAQ system.

Fig. 25. Array of 74 liquid scintillator cells in the bed of the pick-up truck.

Fig. 26. Arrray of liquid scintillator cells showing the location of the Pb bricks in the center of the array.

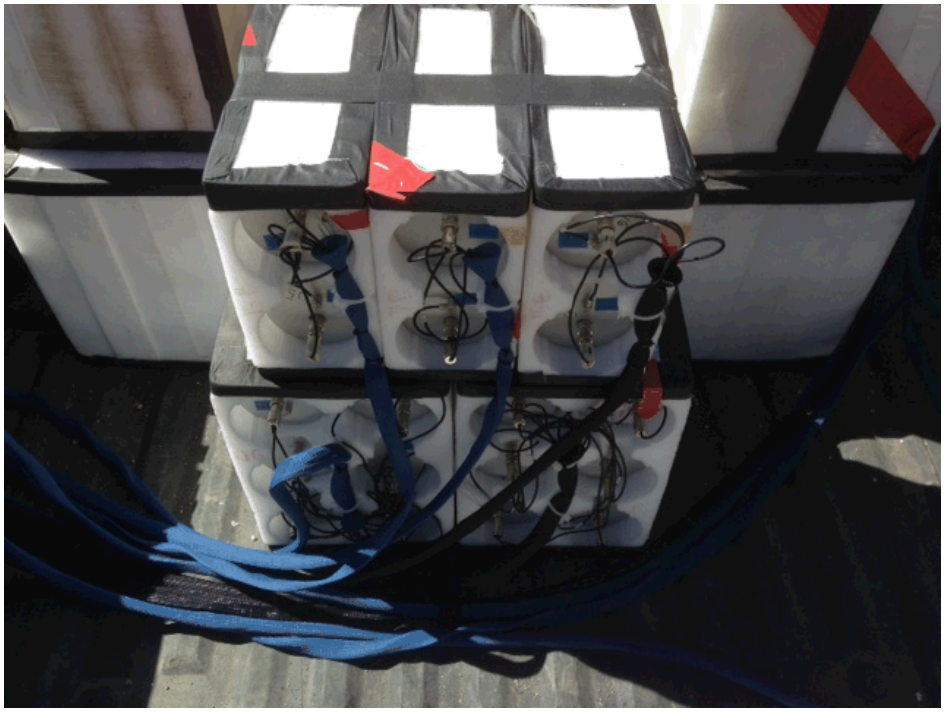

Fig. 27. Close-up of the cable connections to three of the 2-packs and two of the 6-packs of liquid scintillator cells.

Fig. 28. View showing one of the plastic scintillator panels beneath the truck.

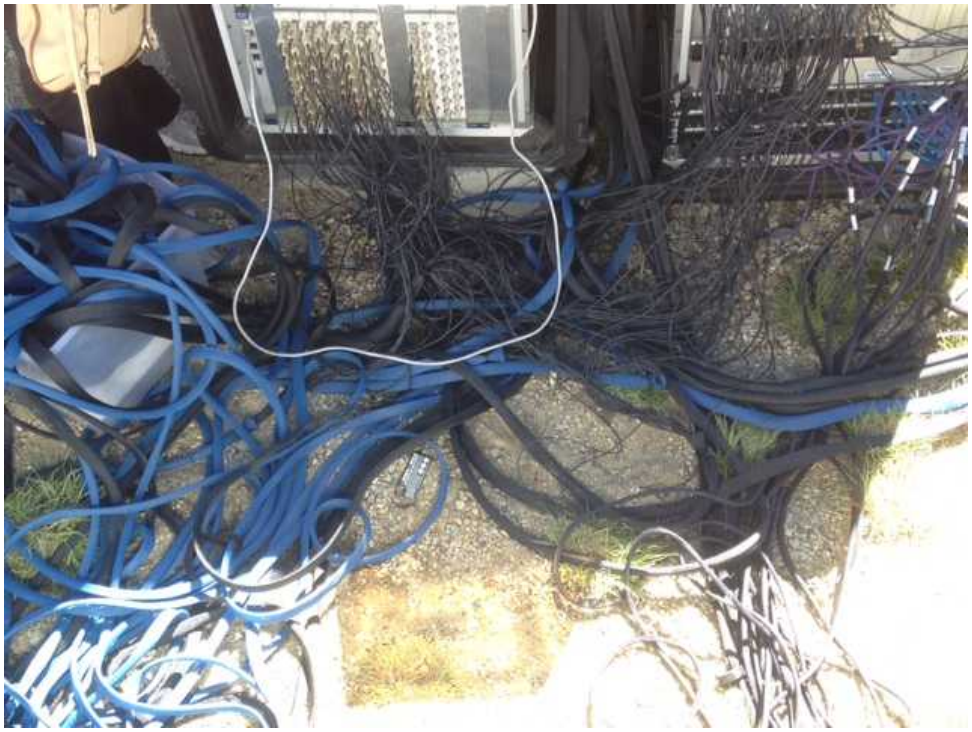

Fig. 29. View showing the connections of the cables to the data acquisition system.

We will now turn to a summary of our experimental observations at White Mountain. Comparisons of the data with Monte Carlo calculations will be reported as part of deliverables for FY15. In Fig. 30 we show a "waterfall" plot showing the time intervals between successive liquid scintillator neutrons gamma rays, and plastic panel MIPs.

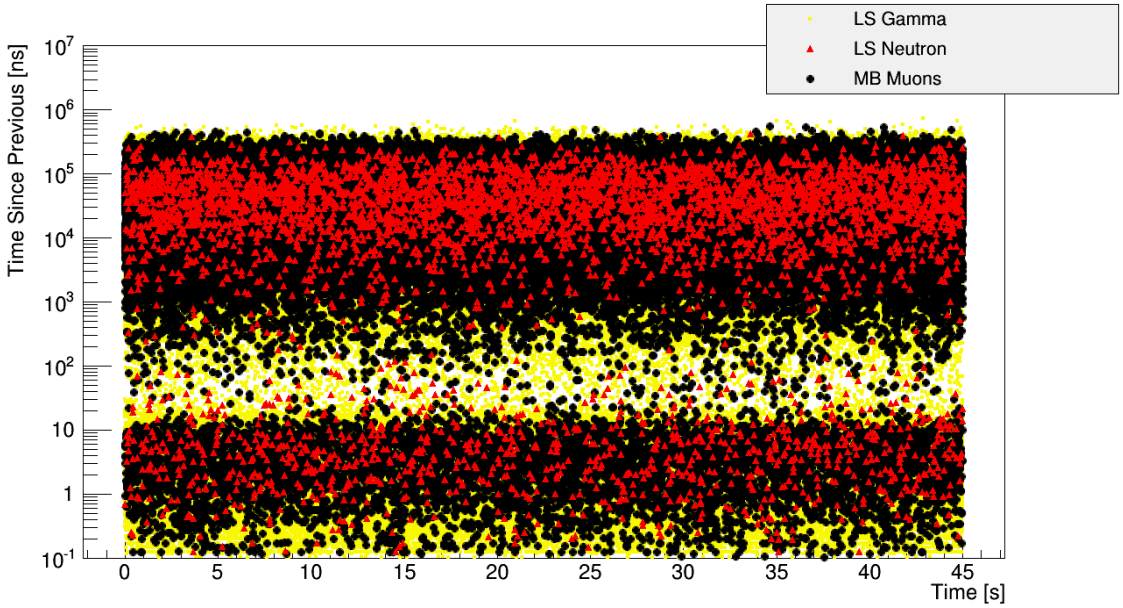

Fig. 30. "Waterfall" plot showing the time interval between successive LS neutrons, LS γ-rays, and plastic scintillator MIP-like signals resulting from cosmic rays interacting with a Pb pile over a time period of 45 seconds.

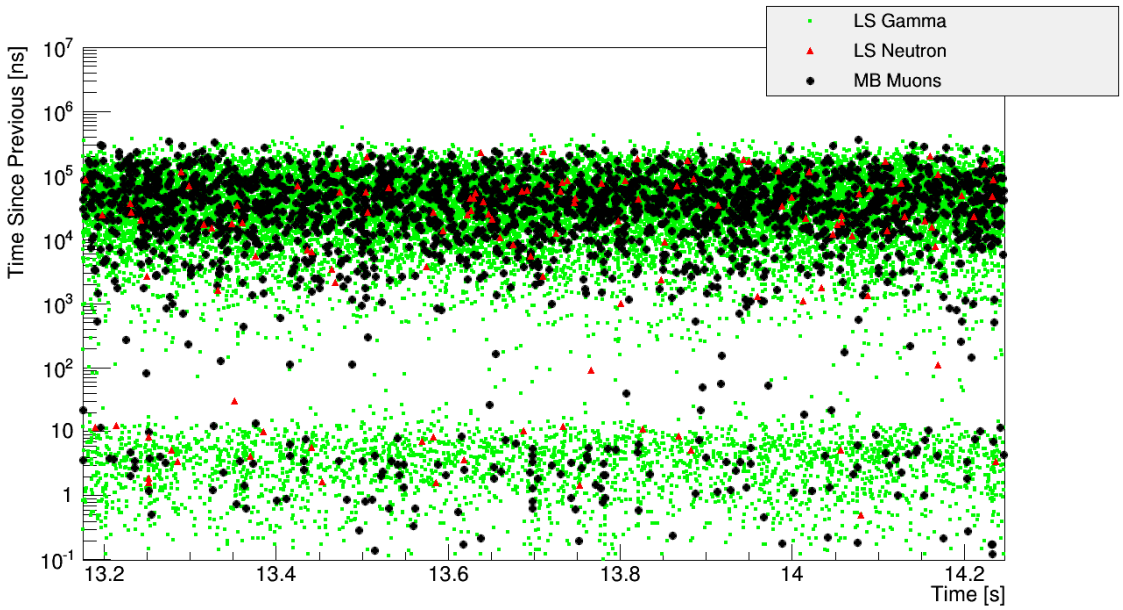

Fig. 31. Blow up of the previous "waterfall" plot showing the time interval between successive liquid scintillator neutrons, liquid scintillator γ-rays, and plastic scintillator MIPS signals resulting from cosmic rays interacting with a Pb pile over a time period of 14 seconds.

As is evident from Fig. 30, the rate of cosmic ray interactions with our detector array at the White Mountain research station is much higher than at sea level. This is to be expected because only 60% of the atmospheric mass lies above the altitude of the White Mountain research station.

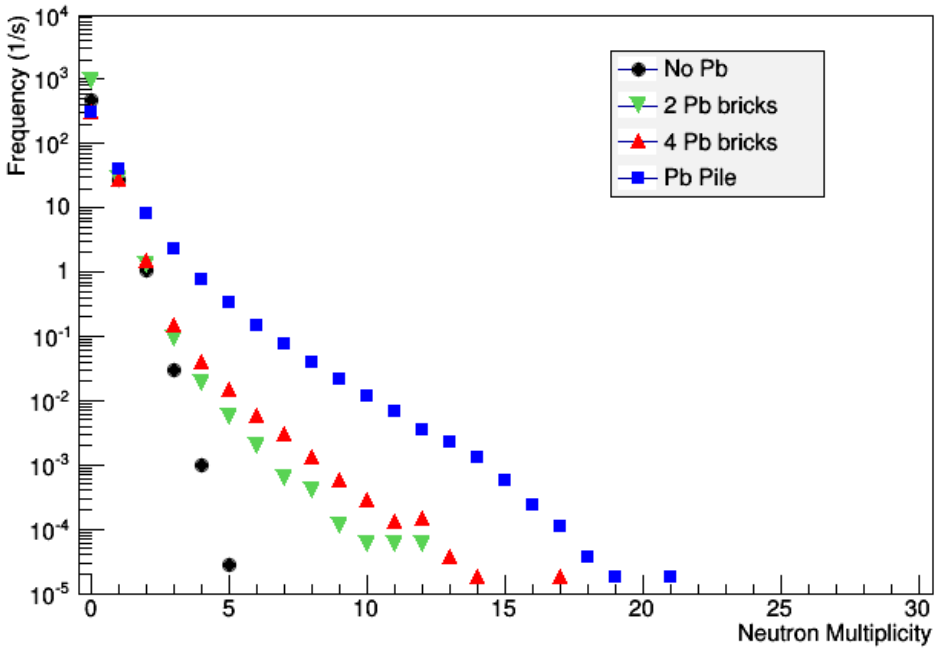

Fig. 302. Fast neutron burst size distribution produced by varying amounts of Pb measured with our array of liquid scintillator cells at the White Mountain Research Station.

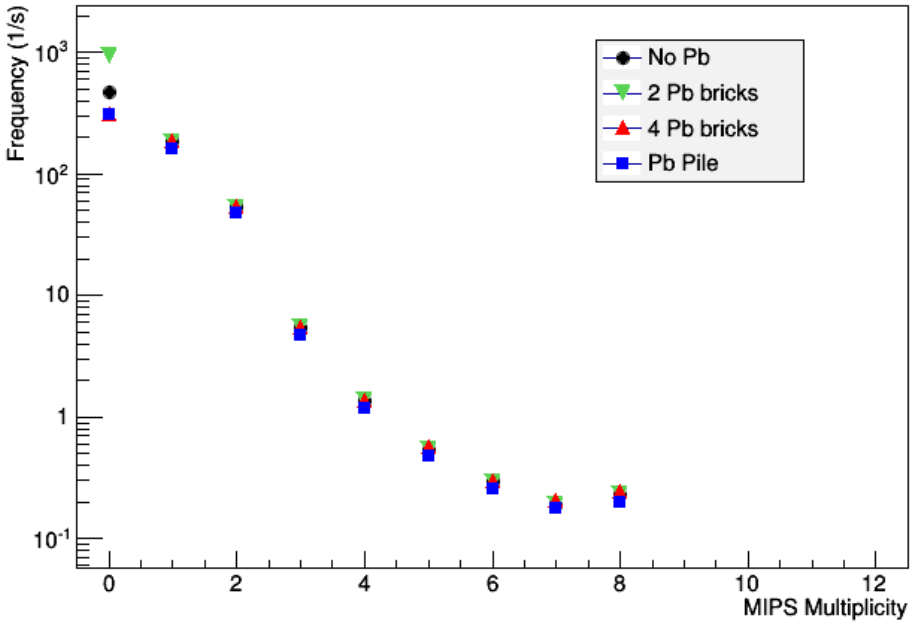

Fig. 33. MIPS burst size distribution measured in the presence of varying amounts of Pb with our plastic scintillator panels at the White Mountain Research Station

We see that, in contrast with the results at LLNL, the MIP-like multiplicity distribution seen at White Mountain is not sensitive to the nearby presence of a Pb pile, not to mention kg quantities of Pb. However this is not true for the correlations between MIP-like signals and liquid scintillator neutrons.

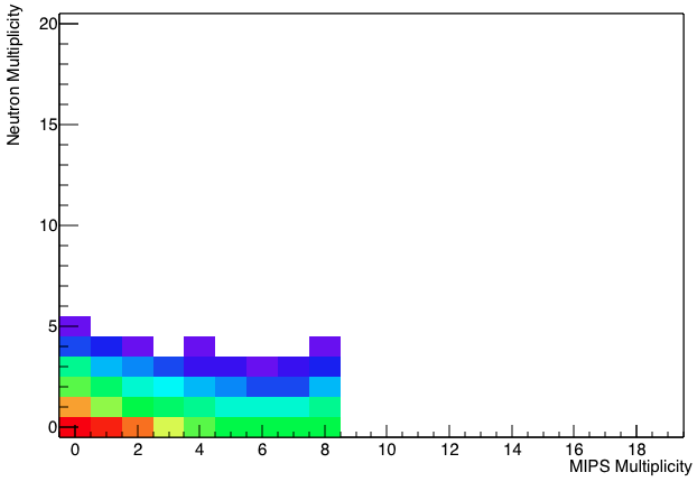

Fig. 35. White Mountain rates for bursts containing multiple LS neutron and/or MIP-like plastic scintillator MIP multiplicities in the absence of a Pb brick pile.

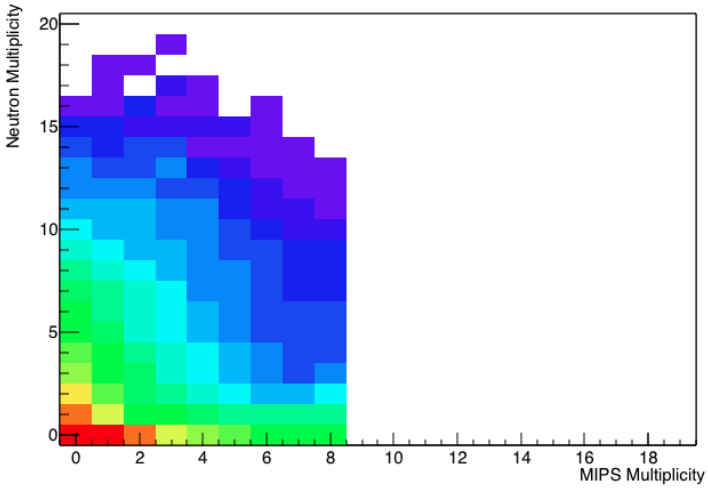

Fig. 36. White Mountain rates for bursts containing multiple LS neutron and/or MIP-like plastic scintillator MIP multiplicities in the presence of a Pb pile.

In Figures 35-36 we show that the presence of the Pb pile strongly enhances the rate for bursts with multiple liquid scintillator and plastic scintillator signals.

Conclusions

The main result of our experiments is that we now have a much better understanding the origin of the unexpected time correlations between the neutron burst signals observed in neutron detectors and MIP-like signals in nearby plastic scintillator detectors. One clue that the plastic scintillator MIP-like signals are associated with the same cosmic ray bursts that produced the Pb pile neutron bursts already evident in our original 2006 experiments is that the time correlations between these two types of signals are strongest for the largest neutron bursts. At the time we surmised that the plastic scintillator signals correlated with the ^{3}He neutron signals were due to secondary cosmic ray muons accompanying the high energy particle responsible for the neutron burst. However, as a result of Monte Carlo simulations of cosmic ray showers we now understand that the correlations between secondary cosmic ray particles are weak because the secondary particles in energetic cosmic ray showers are typically separated by kilometers. On the other hand we have realized that very large bursts of neutrons produced in high Z materials by cosmic rays are rich in neutrons with kinetic energies exceeding 20 MeV. These relatively high energy tertiary

neutrons will be perceived by plastic scintillator detector as a minimum ionizing particle.

These results may also lead to a quantitative understanding of the "ship effect", which is the cold war discovery that ships are prolific sources of neutrons. For example, we expect that high energy secondary cosmic rays will produce large (> 100 neutron) bursts of high energy neutrons in a large steel structure such as a ship. The unexpectedly high rate for these events is a consequence of the fact that although typical cosmic rays at sea level are the result of primary cosmic rays with energies on the order of 10 GeV interacting at the top of the atmosphere, a significant fraction of all cosmic rays reach altitudes as low as a few kilometers before interacting. In addition, primary cosmic rays with energies > 1 TeV will produce secondary particles with energies sufficient to produce large bursts of neutrons. These effects are illustrated in Fig. 37 which illustrates the altitudes of interaction for the primary protons responsible for typical cosmic ray events at sea level and the "ship effect" events associated with high Z materials.

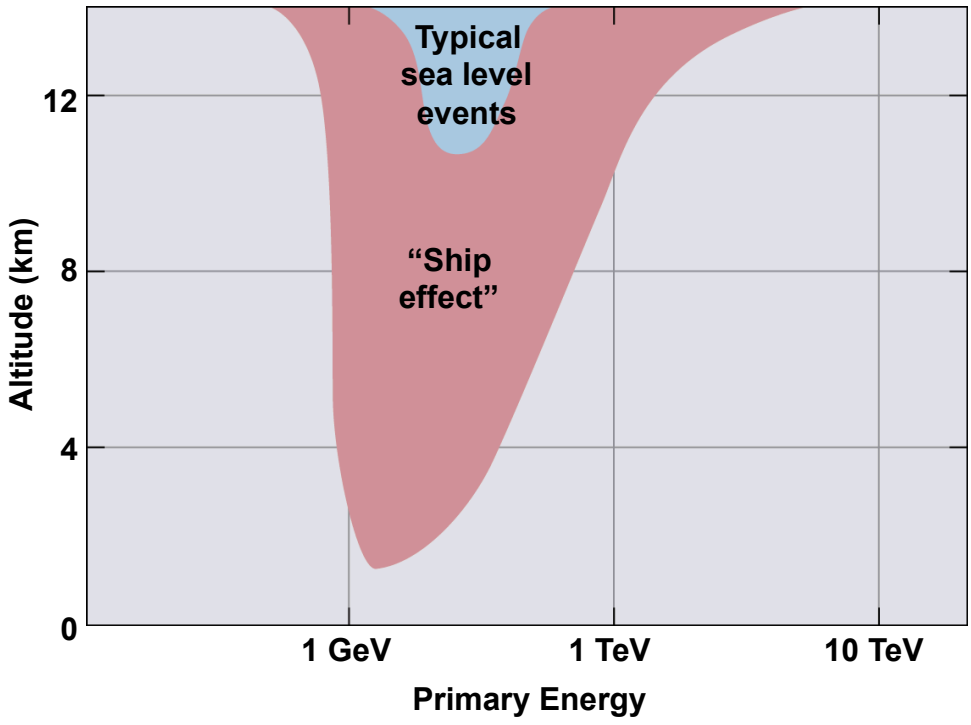

Fig. 37. Typical altitudes of interaction for the primary protons responsible for typical sea level events (blue) and the ship effect (red).